

See discussions, stats, and author profiles for this publication at: <https://www.researchgate.net/publication/1873292>

# Dynamics of Nucleation in the Ising Model

ARTICLE *in* THE JOURNAL OF PHYSICAL CHEMISTRY B · SEPTEMBER 2004

Impact Factor: 3.3 · DOI: 10.1021/jp0471249 · Source: arXiv

---

CITATIONS

83

---

READS

12

2 AUTHORS, INCLUDING:



Albert C Pan

D. E. Shaw Research

32 PUBLICATIONS 1,679 CITATIONS

SEE PROFILE

# Dynamics of Nucleation in the Ising Model

Albert C. Pan and David Chandler

*Department of Chemistry, University of California, Berkeley, CA 94720-1460*

(Dated: February 2, 2008)

Reactive pathways to nucleation in a three-dimensional Ising model at 60% of the critical temperature are studied using transition path sampling of single spin flip Monte Carlo dynamics. Analysis of the transition state ensemble (TSE) indicates that the critical nuclei are rough and anisotropic. The TSE, projected onto the free energy surface characterized by cluster size,  $N$ , and surface area,  $S$ , indicates the significance of other variables in addition to these two traditional reaction coordinates for nucleation. The transmission coefficient,  $\kappa$ , along  $N$  is  $\kappa \approx 0.35$ , and this reduction of the transmission coefficient from unity is explained in terms of the stochastic nature of the dynamic model.

## I. INTRODUCTION

This paper presents a new application of transition path sampling[1, 2, 3, 4], namely to nucleation of bulk phase transitions[5]. It should be of interest to those concerned with computational techniques devoted to rare transitions between metastable states, as well as to those interested in nucleation theory. The application focuses on the simplest example of nucleation, that of a supercooled Ising model. We are not the first to carry out numerical simulations of nucleation in the Ising model. For example, see [6, 7, 8, 9, 10, 11, 12, 13, 14, 15]. Our work is distinguished from these earlier studies in that we focus on the statistics of an ensemble of reactive pathways to nucleation. We are also not the first to use transition path sampling to study nucleation of a bulk phase transition. Zahn, for instance, has used this technique to study atomistic models undergoing solid-solid transitions[16, 17]. That work succeeded at harvesting typical nucleation pathways and examples of transition states for specific molecular systems. In contrast, our focus in this paper is on generic issues raised by recent experiments and simulations[18, 19, 20, 21, 22, 23], issues that suggest the importance of deviations from classical nucleation theory due to fluctuations[6, 24].

The thermodynamics of nucleation are thought to be governed by a competition between two effects in the growing nucleus — an unfavorable contribution from the formation of a surface and a favorable contribution from nucleating the stable phase:

$$\Delta G(N) = -N|\Delta\mu| + N^{\frac{2}{3}}\gamma. \quad (1)$$

Here,  $N$  is the number of particles in the growing nucleus (assumed to be spherical),  $\Delta\mu$  is the chemical potential difference between the two phases and  $\gamma$  is the surface tension (assumed to be that of an infinite planar interface). Equation 1 assumes that the free energy of this non-equilibrium process depends on the size of the growing nucleus as the one relevant variable (i.e. reaction coordinate) that controls its progress: small nuclei tend to shrink due to their large surface area-to-volume ratios while sufficiently large nuclei tend to grow as the bulk free energy dominates. The transition state, or crit-

ical nucleus, then sits atop this free energy barrier between the undercooled and stable phases. This picture is found in any theory that relates the nucleus size to a single reaction coordinate. In general, nucleation, as with all non-equilibrium process, can involve many degrees of freedom[25, 26] and may not be faithfully described by one or even a small handful of coordinates[27, 28].

We investigate to what extent the simplest picture holds. Our analysis involves reversible work calculations, committor distributions, transmission coefficients and, most importantly, the statistics of an ensemble of reactive trajectories. We find that the traditional coordinate,  $N$ , provides a reasonable approximation to the reaction coordinate. But other variables in addition to  $N$  and also cluster surface area,  $S$ , are required for a quantitative treatment. We also find that the critical nuclei in the transition state ensemble are rough and anisotropic as seen recently in experiments on colloidal and polymer systems[18, 19, 20].

## II. MODEL AND SIMULATION DETAILS

Our system is the nearest neighbor Ising model on a cubic lattice with the Hamiltonian:

$$H = -J \sum_{\langle ij \rangle} s_i s_j + h \sum_i s_i \quad (2)$$

where  $J$  ( $> 0$ ) is the coupling constant,  $h$  is the magnetic field and  $s_i$  is a spin variable that can either be 1 or  $-1$ . The bracketed sum over  $i$  and  $j$  denotes a restriction to nearest neighbor pairs. In these simulations, the temperature is 60% of the critical temperature in units of  $J/k_B$  and the field  $h = 0.55$  in units of  $J$ . The lattice has 32 spins on an edge with periodic boundary conditions and is propagated using single spin flip Metropolis Monte Carlo with random site selection. Time is measured in units of sweeps.

The temperature  $0.6 T_c$  is about 20% above the roughening temperature of the three dimensional Ising model,  $T_R$ [29]. One anticipates that below  $T_R$ , the nuclei will tend to be cubic with relatively flat interfaces[11, 12], while above  $T_R$ , nuclei will tend to be isotropic and

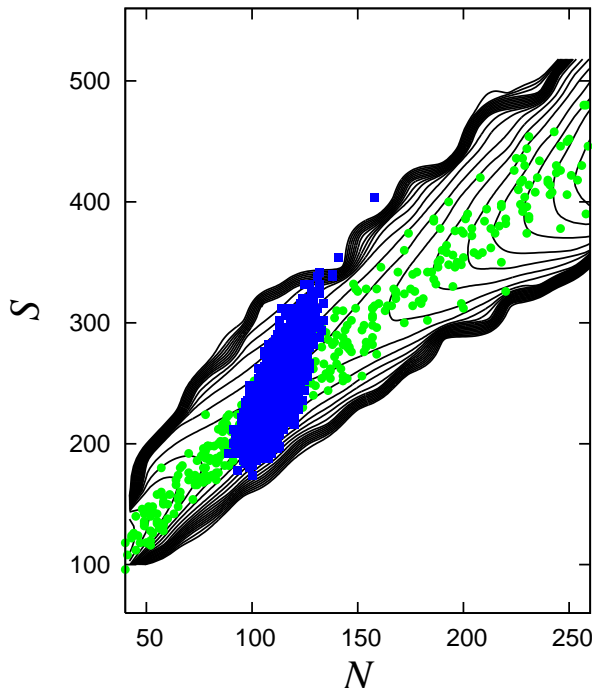


FIG. 1: Contour plot of  $\Delta G(N, S)/k_B T$ , the free energy of a nucleus as a function of its size and surface area. The contour lines are in gradations of  $1 k_B T$ . The green circles show points visited by eight typical trajectories projected onto the  $N$ - $S$  plane. The blue squares show members of the transition state ensemble projected in the same way.

rounded[30]. This latter regime is appropriate for the study of liquid-vapor equilibrium. Using eqn. 1, we can anticipate the typical critical cluster size assuming a spherically isotropic nucleus. Taking  $|\Delta\mu| = 2h$  (due to the usual connections between the Ising spin system and a lattice gas) and  $\gamma \approx 2J$  (assuming the zero temperature value of  $\gamma$  in the Ising model) implies a critical cluster size,  $N^* \sim 200$  with a free energy barrier of about  $40 k_B T$ . In fact, the exact numerical analysis gives  $N^* = 115$  with a corresponding free energy barrier of  $18 k_B T$  (see below). In any case, the size of the critical nucleus is much smaller than our system size and the height of the free energy barrier indicates that nucleation is a rare event.

### III. STATISTICAL ANALYSIS OF AN ENSEMBLE OF REACTIVE TRAJECTORIES

#### A. Transition path sampling

In order to study the dynamics of nucleation without being biased by a particular choice of reaction coordinate, many trajectories of the nucleation event need to be obtained without reference to any specific coordinate. For nucleation, such a calculation might seem difficult to

carry out because the process is a rare event. The difficulty is overcome, however, with transition path sampling (TPS)[3, 4]. In a straightforward simulation, a large majority of computational time is spent simulating the undercooled state even though the nucleation event of interest is fleeting (see, for instance, [31]). In contrast, TPS allows exclusive sampling of the reactive portion of the trajectory. It employs a Monte Carlo walk in the space of reactive trajectories to harvest multiple examples of the rare event without wasting computational time simulating the metastable state. Moreover, no reaction coordinate is required *a priori*.

We apply TPS to nucleation in the Ising model and sample paths connecting nucleated and undercooled states defined by the characteristic functions  $h_A(q)$  and  $h_B(q)$ :

$$h_A(q) = \begin{cases} 1, & N(q) < N_A \\ 0, & N(q) > N_A \end{cases} \quad (3)$$

$$h_B(q) = \begin{cases} 0, & N(q) < N_B \\ 1, & N(q) > N_B \end{cases} \quad (4)$$

Here,  $q = (s_1, s_2, \dots, s_i, \dots)$  denotes a particular configuration of the lattice and  $N(q)$  returns the size of the largest cluster in that configuration. The limits,  $N_A$  and  $N_B$  are far removed from the transition state region. In other words,  $h_B(q)$  gives a signal if a configuration is in the product region and  $h_A(q)$  gives a signal if a configuration is in the reactant region. In this calculation,  $N_A = 26$  and  $N_B = 260$  are chosen such that the free energy barrier in FIG. 5 (see below) separating the two basins exceeds  $10 k_B T$ . This ensures that once a configuration finds itself in either the reactant or product region, it remains there for times much longer than the molecular relaxation time and that the reactant and product basins do not overlap. Since  $N$  may not necessarily be an adequate reaction coordinate, we verify this latter condition by separate simulations of configurations starting in both regions.

In these simulations, trajectories 150 time units in length are sampled with the shooting algorithm[2, 4]: a time slice is chosen at random from a trial trajectory and then new forward and backward paths are generated using the underlying dynamics of the system. The newly

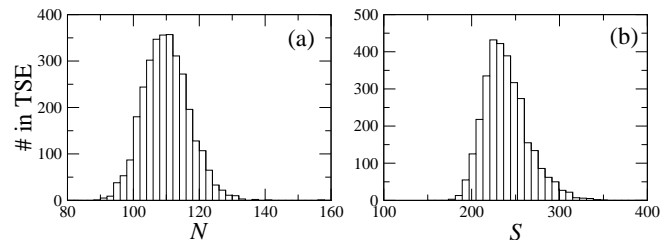


FIG. 2: Distributions of cluster sizes (a) and surface areas (b) in the transition state ensemble. The average values from the two histograms are  $N = 110$  and  $S = 241$ .

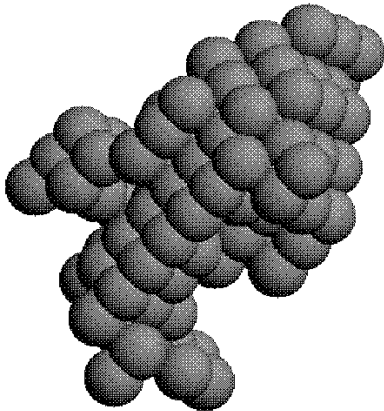


FIG. 3: A characteristic example from the transition state ensemble. The spheres represent nucleated spins on the cubic Ising lattice.

generated trajectory is accepted if it connects the reactant and product regions defined by the characteristic functions  $h_A(q)$  and  $h_B(q)$ . Since the dynamics of this system are stochastic, a new path can be generated by simply shooting one direction at a time, as the forward and backward transition probabilities are equal[4]. This increases the acceptance probability. A complete shooting move is defined as two such moves. We relax an initial trajectory[32] with 25,000 moves and then 1,000 independent trajectories are harvested, one every 100 moves. Convergence and adequate choice of path length are verified by calculation of  $\langle h_B[q(t)] \rangle_{AB}$ , the characteristic function  $h_B(q)$  along a reactive trajectory averaged over the transition path ensemble (not shown). The fact that this quantity reaches the linear regime implies that our path length is long enough to sample typical barrier crossing behavior[4].

One often imagines that the most important reaction coordinate describing nucleation is the size of the growing cluster,  $N$ , as alluded to in the Introduction. Another relevant, but secondary, reaction coordinate which is also considered is the cluster's surface area,  $S$ . In FIG. 1, we project paths obtained from TPS onto a contour plot of the  $N$ - $S$  free energy (green circles).

The free energy surface in FIG. 1 is determined using umbrella sampling with hard wall constraints[33]. For this and all subsequent calculations, a set of spins is considered a nucleus of size  $N$  if each spin in the set is a nearest neighbor of at least one other spin in the set. The surface area,  $S$ , of such a cluster is the number of exposed faces. The umbrella sampling windows constrain the size

and surface area of the *largest* cluster in a given configuration of the lattice. For  $N > 20$ , it is highly unlikely that there is more than one cluster of that size in any given configuration of the full system. Approximately 200 overlapping windows of average size  $\Delta N = 12$  by  $\Delta S = 40$  are used. In each window, an initial configuration is equilibrated for 50,000 sweeps and statistics are taken over a subsequent run of 200,000 sweeps. The windows are linked together with multiple histograms generalized to two dimensions[34].

## B. The transition state ensemble

A configuration is considered a member of the transition state ensemble (TSE) if half of the new trajectories initiated from it cause the nucleus to shrink and the other half cause it to grow. From the 1,000 trajectories acquired through transition path sampling, we found approximately 3,200 members of the TSE.

To determine transition states with a minimum of computational effort, we check each configuration along a reactive trajectory in the following way[4]. (1) If a configuration is in either the reactant or product region, it is rejected as a transition state candidate straight away. (2) If a configuration is not in the reactant or product region, a series of additional trajectories are initiated from that configuration and  $p_B$ , the ratio of paths which end up in region  $B$  to the total number of paths initiated, is calculated after 11, 14, 17, 20, 25, 30, 35, 42 and 49 trajectories[35]. After the 49th trajectory, additional trajectories are generated up to a maximum of 100 trajectories, and  $p_B$  is calculated after every trajectory. The configuration is rejected as a transition state candidate if  $p_B$  falls outside the 95% confidence interval around  $p_B = 0.5$  at any point. Finally, (3) if  $p_B = 0.5$  within 95% confidence after 100 trajectories, then that config-

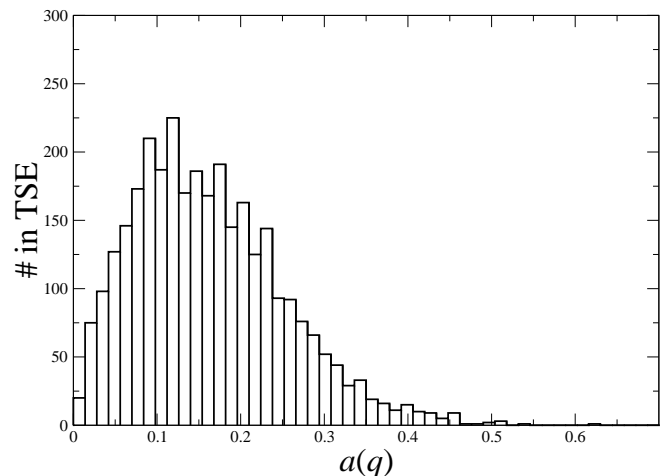


FIG. 4: The distribution of  $a(q)$ , a function of the principal moments of inertia of the nuclei (see eqn. 5), in the transition state ensemble.

uration is accepted as a member of the transition state ensemble.

FIG. (1) juxtaposes projections onto the  $N$ - $S$  plane of representative trajectories and the TSE with the corresponding free energy surface. The comparisons indicate that  $N$  and  $S$  capture much of the mechanism for nucleation. The TSE is not perpendicular to the  $N$  axis, showing that  $S$  as well as  $N$  is important to the mechanism of nucleation. The comparisons also show that other variables in addition to  $N$  and  $S$  play significant roles in the mechanism. In particular, the orientation of the projected TSE is far from that expected from the saddle in the free energy surface. Further, the projected TSE has a significant width.

Further analysis of the TSE shows that the critical nuclei are rough and anisotropic. The distribution of cluster sizes in the transition state ensemble is shown in FIG. 2(a). A typical critical nucleus taken from the transition state ensemble is shown in FIG. 3. The anisotropy and roughness of this nucleus are characteristic of the transition state ensemble. Quantitative measurements of this fact are shown in FIG. 2(b) and FIG. 4. FIG. 2(b) shows the distribution of surface areas in the transition state ensemble. The average surface area is 241 compared to an average cluster size of 110 (FIG. 2). This observed average surface area is almost 30% larger than would be expected of a compact spherical cluster of 110 particles indicating that the critical nuclei are, on average, extremely rough[36].

FIG. 4 shows the distribution of the anisotropy function,

$$a(q) = \frac{I_1(q)}{I_2(q)} - 1, \quad (5)$$

where  $I_1(q)$  and  $I_2(q)$  are the largest and second largest, respectively, principal moments of inertia. For a completely isotropic structure,  $a(q) = 0$ . The deviation from zero indicates anisotropy. In contrast, the equilibrium average crystal shape for a nearest neighbor three-dimensional Ising model above the roughening transition is isotropic and rounded[30].

In the following sections, we contrast these results obtained from the statistical analysis of an ensemble of reactive trajectories with those obtained from more conventional methods.

#### IV. CLUSTER SIZE AS REACTION COORDINATE

##### A. Reversible work of cluster formation

FIG. 5 shows the free energy  $\Delta G(N)$  where, within an additive constant,  $\Delta G(N) = -k_B T \sum_S \exp[-\Delta G(S, N)]$ . Qualitatively, we see that the computed curve resembles the curve predicted by equation 1. The maximum occurs at  $N^* = 115$  monomers where  $\Delta G(N^*)$  is within a small fraction of

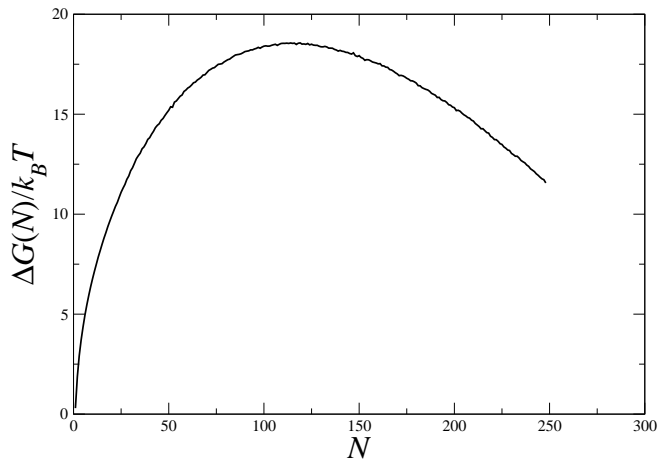


FIG. 5: The free energy of a growing cluster in the three-dimensional Ising model at  $T = 0.6 T_c$  and  $h = 0.55 J$ .

$k_B T$  from the free energy at  $N = 110$  monomers, the average of  $N$  in the TSE.

The free energy in FIG. 5 is calculated using umbrella sampling with hard wall constraints, and different umbrella windows are linked together using the multiple histogram method. Approximately 30 overlapping windows of size  $\Delta N = 12$  are used. In each window, an initial configuration is equilibrated with 50,000 sweeps and then statistics are taken over a run of 100,000 sweeps.

##### B. Committor distribution

The extent to which  $\Delta G(N)$  provides an adequate indication of the dynamics can be determined by calculating the probability that configurations constrained to have a nucleus of size  $N^*$  will either grow or shrink. If  $N$  is

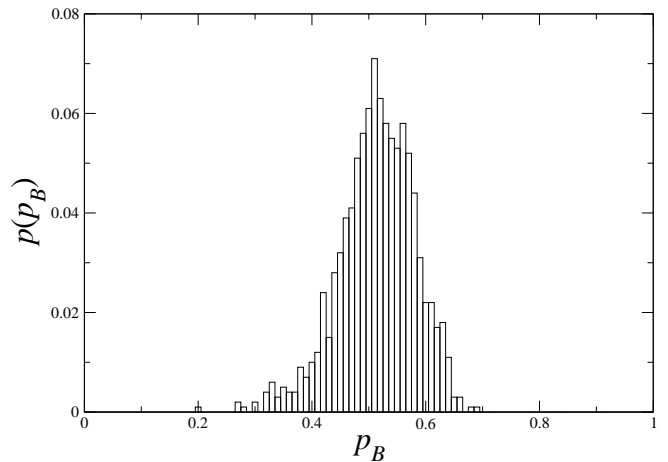


FIG. 6: Committor distribution with cluster size  $N$  constrained to  $N^*$ . The distribution is peaked around  $p_B = 50\%$  indicating that  $N$  is a reasonable reaction coordinate for this process.

indeed a good reaction coordinate, a configuration with an  $N^*$  sized nucleus should be just as likely to grow as to shrink. In this case, the probability distribution, also called a committor distribution, would be peaked around 50% [3, 4].

The distribution in FIG. 6 represents the results of such a calculation where  $p_B$  once again denotes the probability of a configuration ending up in the product region. A set of 1,000 independent configurations is drawn from the ensemble of configurations constrained to have  $N = N^*$  and 200 separate trajectories are then run for each configuration. The final configuration of these trajectories is then judged by the characteristic function  $h_B(q)$  (eqn. 4).

The fact that the committor distribution for  $N$  constrained to  $N^*$  is peaked around 50% indicates that it is a reasonable approximation to the reaction coordinate for nucleation. If this were not the case, we would expect a different distribution (see, for example, [28]). The spread in the distribution, however, indicates that coordinates other than  $N$  are still involved albeit in a secondary way.

### C. The transmission coefficient along $N$

We calculate the transmission coefficient,  $\kappa$ , via the reactive flux method [22, 33, 37]. The value of  $\kappa$  is then given by the plateau of the normalized reactive flux correlation function:

$$k(t) = \frac{\langle \dot{N}(0) \theta[N(t) - N^*] \rangle'}{\langle \dot{N}(0) \theta[\dot{N}(0)] \rangle'} \quad (6)$$

where  $\theta$  is the Heaviside step function,  $N(t)$  is shorthand for  $N[q(t)]$ , and the primed angled brackets indicate an equilibrium average with  $N(0)$  constrained to  $N^*$ . In other words, we constrain our ensemble of initial states to be at the maximum,  $N^*$ , of  $\Delta G(N)$  (FIG. 5).

A plot of  $k(t)$  is given in FIG. 7. A plateau value of  $\kappa < 1$  along  $N$  is an indicator of recrossings due to friction in the barrier region. Here,  $\kappa \approx 0.35$ . We argue below that the friction in our system is mainly a manifestation of the stochastic dynamics in the Monte Carlo trajectory.

For the calculations in FIG. 7, a set of independent configurations is drawn from the ensemble of configurations constrained to have  $N = N^*$  and trajectories are run beginning from these configurations. The reactive flux correlation function,  $k(t)$ , is then calculated as an average over these trajectories. The initial velocity of the reaction coordinate,  $\dot{N}(0)$ , is taken to be the finite difference,  $N(1) - N(0)$ .

### D. Friction from stochastic dynamics

The friction which reduces the value of the transmission coefficient in this case can be attributed mostly to

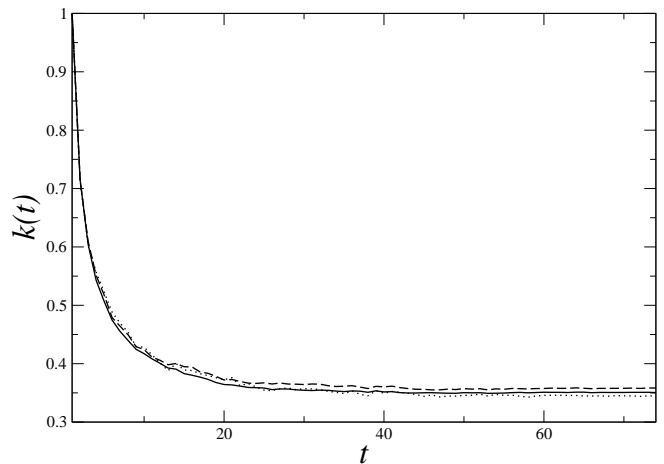


FIG. 7: Plot of  $k(t)$  (eqn. 6), where time is measured in Monte Carlo sweeps. The dotted, dashed and solid lines are averages over 10,000, 30,000 and 80,000 trajectories, respectively.

the diffusive nature of a random walk on a relatively flat barrier top. To illustrate this idea, we consider a random walk beginning at the top of a free energy barrier and calculate its transmission coefficient. Here, we assume that the random walker makes uncorrelated steps of typical length  $\delta N$  and is committed to a basin once it has traveled a distance  $l$  corresponding to when the free energy has changed by  $\sim 1 k_B T$  relative to the barrier top. The length  $l$  therefore depends on the curvature of the barrier near its maximum.

The reactive flux correlation function in eqn. (6) can be thought of as a ratio of the average flux across the dividing surface of trajectories which end up in the product region to the average flux across the dividing surface of trajectories with an initial positive flux (i.e. toward the product region). For a random walk process, these quantities can be evaluated analytically from a straightforward application of binomial statistics. The quantity of interest is the value of the transmission coefficient  $\kappa(M)$  where  $M \sim l/\delta N$  is the number of steps required to fall a distance  $1 k_B T$  in free energy from the barrier top. If  $M = 1$ , there are only two possible trajectories — one with positive initial flux which is trapped on the positive side of the dividing surface and one with initial negative flux which is trapped on the negative side. In this case, we see that  $\kappa(1) = 1$ . Similarly for  $M = 2$ , out of four possible trajectories, one trajectory is trapped on the positive side of the dividing surface with initial positive flux, one trajectory is trapped on the negative side with initial negative flux, and the other two trajectories end up back at the dividing surface, one with positive initial flux and one with negative initial flux. In this case,  $\kappa(2) = 1/2$ . In general, we see that the denominator of  $\kappa(M)$  is half of all possible trajectories of length  $M$  and that the numerator is, within the subset of trajectories of length  $M$  which end up in the product region, the number with a positive initial flux minus the number with a

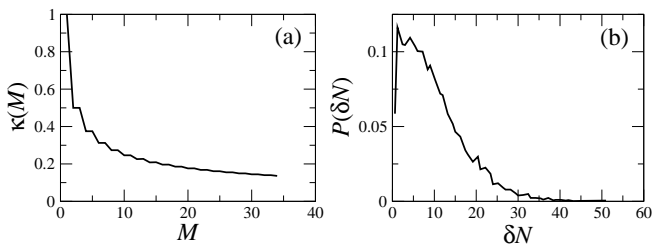


FIG. 8: (a) The transmission coefficient  $\kappa$  for a random walker as a function of the number of steps  $M$  required for it to fall off the barrier top. (b) Probability of observing a change in the nucleus size,  $\delta N$  after one sweep of the lattice in the region  $1 k_B T$  around the barrier top in FIG. 5,  $N \in [80, 160]$  (averaged over 500 trajectories).

negative initial flux. Therefore, for arbitrary (even)  $M$ , we have:

$$\kappa(M) = n(M)/d(M) \quad (7)$$

where,

$$d(M) = \frac{1}{2} \sum_{r=0}^M \binom{M}{r}, \quad (8)$$

and, for even  $M$ ,

$$n(M) = 1 + \sum_{r=1}^{M/2-1} \left[ \binom{M-1}{r} - \binom{M-1}{r-1} \right] \quad (9)$$

with  $\binom{i}{j} = i!/(i-j)!j!$ , as usual. For odd  $M$ , the result is the same except the upper limit in the sum giving  $n(M)$  is changed to  $(M-1)/2$ .  $\kappa(M)$  is plotted in FIG. 8(a). For the transmission coefficient of nucleation, the distance to  $1 k_B T$  from the barrier top is  $l \sim 45$  and the typical random walk step size is  $\delta N \sim 11$ . The latter result can be arrived at by considering the typical size of fluctuations of a nucleus of size  $N^*$ . In this case,

$\delta N \sim \sqrt{N^*} \sim 11$ . Alternatively, one can compute the probability of observing a change,  $\delta N$ , in the nucleus size after one sweep. This probability, depicted in FIG. 8(b), shows that  $\delta N \sim 11$  is a reasonable estimate. These numbers imply that the typical random walk step size is approximately 4 which gives  $M \sim (l/\delta N)^2 \sim 16$ . This leads to an estimate of  $\kappa \approx 0.20$ . Considering the rough nature of the approximation, this result is close to the simulation result of  $\kappa \approx 0.35$  indicating that the stochastic nature of the dynamics is really playing the major role in determining the value of the transmission coefficient along  $N$ .

Zeldovich was the first to write down an analytic expression for the transmission coefficient,  $Z$ , for nucleation[38]:

$$Z = \left\{ \frac{1}{2\pi} \left[ \frac{\partial^2(\Delta G(N)/k_B T)}{\partial N^2} \right]_{N^*} \right\}^{1/2} \quad (10)$$

This factor, a measure of the barrier width, is an indication of the diffusive nature of nucleation dynamics. In a more modern context, we see that  $Z$  is proportional to the high friction limit of Kramers expression for  $\kappa$ [39]. The Zeldovich factor has units of  $1/N$  and therefore depends also on the size of the nucleus' typical fluctuations. In our system,  $Z \approx 0.013$ , which, when multiplied by  $\delta N \sim 11$ , gives a reasonable estimate of  $\kappa \approx 0.14$ .

An atomistic simulation study of liquid-gas nucleation gives a value of  $\kappa$  two orders of magnitude smaller than 0.35[23]. The coarse grained dynamics used in the current study takes much larger steps in configuration space than atomistic dynamics. The corresponding  $M$  for the atomistic dynamics is thus much larger than that which we associate with the Monte Carlo random walk. The much larger value of  $M$  can explain the much smaller value of  $\kappa$ , as eqn. 7 shows.

The authors thank Pieter Rein ten Wolde for discussions and advice on this work, which has been supported by the US National Science Foundation. A.C.P. is a NSF Graduate Research Fellow.

- 
- [1] Dellago, C.; Bolhuis, P.; Csajka, F.; Chandler, D. *J. Chem. Phys.* **1998**, *108*, 1964.
  - [2] Dellago, C.; Bolhuis, P.; Chandler, D. *J. Chem. Phys.* **1998**, *108*, 9236.
  - [3] Bolhuis, P. G.; Dellago, C.; Chandler, D.; Geissler, P. *Ann. Rev. of Phys. Chem.* **2002**, *59*, 291.
  - [4] Dellago, C.; Bolhuis, P. G.; Geissler, P. L. *Transition Path Sampling. In Advances in Chemical Physics*; Wiley: 2001.
  - [5] Oxtoby, D. W. *J. Phys.: Condens. Matter* **1992**, *4*, 7627-7650.
  - [6] Binder, K.; Müller-Krumbhaar, H. *Phys. Rev. B* **1974**, *9*, 2328.
  - [7] Marro, J.; Bortz, A. B.; Kalos, M. H.; Lebowitz, J. L. *Phys. Rev. B* **1975**, *12*, 2000.
  - [8] Sur, A.; Lebowitz, J. L.; Marro, J.; Kalos, M. H. *Phys. Rev. B* **1977**, *15*, 3014.
  - [9] Stauffer, D.; Coniglio, A.; Heermann, D. W. *Phys. Rev. Lett.* **1982**, *49*, 1299.
  - [10] Heermann, D. W.; Coniglio, A.; Klein, W.; Stauffer, D. *J. Stat. Phys.* **1984**, *36*, 447.
  - [11] Wonczak, S.; Strey, R.; Stauffer, D. *J. Chem. Phys.* **2000**, *113*, 1976.
  - [12] Stauffer, D. *Int. J. Mod. Phys. C* **1999**, *10*, 809.
  - [13] Schmeltzer, J.; Landau, D. P. *Int. J. Mod. Phys. C* **2001**, *12*, 345.
  - [14] Shneidman, V. A.; Jackson, K. A.; Beatty, K. M. *J. Chem. Phys.* **1999**, *111*, 6932.
  - [15] Shneidman, V. A.; Jackson, K. A.; Beatty, K. M. *Phys. Rev. B* **1999**, *59*, 3579.

- [16] Zahn, D.; Leoni, S. *Phys. Rev. Lett.* **2004**, *92*, 250201-1.
- [17] Zahn, D. *J. Solid State Chem.* **2004**, (in press).
- [18] Balsara, N. P.; Lin, C.; Hammouda, B. *Phys. Rev. Lett.* **1996**, *77*, 3847-3850.
- [19] Lefebvre, A. A.; Lee, J. H.; Jeon, S. H.; Balsara, N. P.; Hammouda, B. *J. Chem. Phys.* **1999**, *111*, 6082-6099.
- [20] Gasser, U.; Weeks, E. R.; Schofield, A.; Pusey, P.; Weitz, D. *Science* **2001**, *292*, 258-262.
- [21] ten Wolde, P. R.; Ruiz-Montero, M. J.; Frenkel, D. *J. Chem. Phys.* **1996**, *104*, 9932.
- [22] ten Wolde, P. R.; Frenkel, D. *J. Chem. Phys.* **1998**, *109*, 9901-9918.
- [23] ten Wolde, P. R.; Ruiz-Montero, M. J.; Frenkel, D. *J. Chem. Phys.* **1999**, *110*, 1591-1599.
- [24] Binder, K.; Stauffer, D. *J. Stat. Phys.* **1972**, *6*, 49.
- [25] Langer, J. S. *Ann. Phys.* **1969**, *54*, 258.
- [26] Binder, K.; Stauffer, D. *Adv. Phys.* **1976**, *25*, 343.
- [27] Bolhuis, P. G.; Dellago, C.; Chandler, D. *Proceedings of the National Academy of Sciences* **2000**, *97*, 5877.
- [28] Geissler, P. L.; Dellago, C.; Chandler, D. *J. Phys. Chem. B* **1999**, *103*, 3706-3710.
- [29] Weeks, J. D.; Gilmer, G. H.; Leamy, H. J. *Phys. Rev. Lett.* **1973**, *31*, 549.
- [30] Rottman, C.; Wortis, M. *Phys. Rev. B* **1984**, *29*, 3287.
- [31] Matsumoto, M.; Saito, S.; Ohmine, I. *Nature* **2002**, *416*, 409-414.
- [32] The initial trajectory was generated by taking a configuration with  $N = N^*$  generated during umbrella sampling and running trajectories until a path was found connecting the reactant and product basins. Even though this path may have been highly unphysical, subsequent relaxation through shooting moves, analogous to Monte Carlo relaxation of an initial state before sampling, equilibrated the path.
- [33] Chandler, D. *Introduction to Modern Statistical Mechanics*; Oxford University Press: 1987.
- [34] Frenkel, D.; Smit, B. *Understanding Molecular Simulation: From Algorithms to Applications*; Academic Press: 1996.
- [35] McCormick, T. A. *Dynamics of Complex System*, Thesis, University of California, Berkeley, 2002 Modeling the calculation of  $p_B$  as a binomial process, McCormick determined the fraction  $f(n)$  of true transition states that are calculated to have a value of  $p_B$  statistically different from 0.5 after  $n$  trial trajectories (i.e. the fraction of true transition states that might be missed as members of the TSE). At small values of  $n$ ,  $f(n)$  fluctuates as much as 10 – 20% as  $n$  is varied. The numbers 11, 14, 17, 20, 25, 30, 35, 42 and 49 were chosen at the minima of  $f(n)$  for  $n < 50$ .
- [36] The minimal surface area for a nucleus of size  $N$  was calculated by creating a compact spherical cluster with  $N$  monomers on a three dimensional Ising lattice and determining its surface area.
- [37] Chandler, D. *J. Chem. Phys.* **1978**, *68*, 2959.
- [38] Frenkel, J. *Kinetic Theory of Liquids*; Dover: 1955 See chapter VII, section 4.
- [39] Hänggi, P.; Talkner, P.; Borkovec, M. *Rev. Mod. Phys.* **1990**, *62*,.